

Coherent nonlinear pulse propagation on a free-exciton resonance in a semiconductor

N. C. Nielsen, S. Linden, and J. Kuhl

Max-Planck-Institut für Festkörperforschung, D-70569 Stuttgart, Germany

J. Förstner and A. Knorr

Institut für Theoretische Physik, Technische Universität Berlin, D-10623 Berlin, Germany

S. W. Koch and H. Giessen*

Department of Physics and Material Sciences Center, Philipps-Universität, D-35032 Marburg, Germany

(Received 4 July 2001; published 14 November 2001)

The coherent exciton-light coupling in pulse propagation experiments on the *A*-exciton resonance in bulk CdSe is investigated over a broad intensity range. At low light intensities, polariton propagation beats due to interference between excited states on both polariton branches are observed. In an intermediate intensity regime, the temporal polariton beating is suppressed in consequence of exciton-exciton interaction. At the highest light intensities, self-induced transmission and multiple pulse breakup are identified as a signature for carrier density Rabi flopping. Exciton-phonon scattering is shown to gradually eliminate coherent nonlinear propagation effects due to enhanced dephasing of the excitonic polarization. Calculations using the semiconductor Maxwell-Bloch equations are in qualitative agreement with the experimental data.

DOI: 10.1103/PhysRevB.64.245202

PACS number(s): 78.47.+p, 42.50.Md, 78.20.Bh, 71.35.Gg

I. INTRODUCTION

The investigation of pulse propagation through opaque materials is of great importance for the understanding of coherent nonlinear light-matter interaction. While the associated optical effects are well established in atomic and molecular vapors—which can be modeled by noninteracting two-level systems^{1,2}—the situation is substantially modified in semiconductors due to the Coulomb interaction between optically generated electron-hole excitations.^{3–5} However, many of the familiar coherent transient two-level phenomena such as free induction decay, photon echo, and Rabi flopping have been rediscovered in semiconductors.^{3,4,6} For bound excitons in CdS, which are well approximated by noninteracting two-level systems, even the appearance of self-induced transparency (SIT) has been detected several years ago.⁷ On the other hand, spatial dispersion⁸ and excitation-induced nonlinearities of the free-exciton resonance⁶ give rise to striking differences of the optical response in semiconductors when compared with idealized two-level systems. In particular, numerical studies of pulse propagation in semiconductors came to the conclusion that these many-body effects may prevent the establishment of complete SIT on free-exciton resonances in condensed matter.⁹ Only within simplified model systems, the phenomenon of excitonic SIT in resonantly excited semiconductors can be investigated analytically.¹⁰ Nevertheless, Rabi flopping of the carrier density, coherent long-distance propagation, and a high degree of transmission have been predicted.^{11,12} This so-called self-induced transmission regime was recently discovered on the free-exciton resonance in CdSe.¹³

In this paper, we present a comprehensive analysis of subpicosecond pulse propagation on the *A*-exciton resonance of CdSe. Our work clearly identifies coherent exciton-light coupling over a broad intensity range and permits comparison with numerical calculations based on the semiconductor

Maxwell-Bloch equations. The increase of the signal-to-noise ratio by approximately one order of magnitude as compared to the data of Ref. 13 reveals interesting novel features of coherent light-matter interaction. In particular, we were able to determine the pulse delay and the effective propagation velocity in dependence on the pulse intensity and to measure the increasing suppression of coherent nonlinear pulse propagation in the presence of phase-destroying exciton-phonon scattering.

II. THEORETICAL BACKGROUND

In this section, we summarize known facts on pulse propagation in semiconductor bulk material and outline their theoretical description. The transition from linear to nonlinear optical phenomena around the band edge of a semiconductor occurs if the density of optically generated excitons is large enough to allow interaction processes between them.

At low light intensities, the interaction between the optically generated excitons can be neglected. In this case, the exciton-light system forms new quasiparticles, so-called exciton-polaritons.¹⁴ The exciton-radiation coupling causes an anticrossing between the dispersion relations of the exciton and light, thus splitting the polariton dispersion into an upper and lower branch. If the frequency spectrum of a resonant short pulse coherently excites a broad range of modes on both branches, the interference of the excited polaritons at the end of the sample results in the formation of a pulse tail whose shape exhibits a pronounced nonperiodic temporal beating. Several periods of this polariton beating have been observed experimentally and proved excellent agreement with linear dispersion theory for the excitonic resonance.¹⁵ However, at increased pulse intensities, the polariton beating is found to be suppressed due to incoherent exciton-exciton interaction which yields dephasing of the excitonic polarization. Experimentally, this suppression can be realized via a

faster decay of the propagated pulse tail as well as a reduction of the beat modulation depth.¹⁶ Upon further increase of the intensity, a new type of propagation-induced pulse shape oscillations occurs. These oscillations are due to Rabi flopping of the carrier density. The corresponding temporally interchanging absorption and gain during a full flopping period cause modulations on the initial pulse shape.¹³

To describe the pulse shape modulations over the whole intensity regime, the transition between the linear and the nonlinear optical response must be treated theoretically. This can be done by using material equations that describe the temporal and spatial evolution of the material polarization and adding a wave equation for the calculation of the optical field. While the dynamics of the optical field can be calculated within the full wave¹⁷ or the reduced wave equation,^{9,18} the corresponding polarization, which acts as a source term in the wave equation, is calculated by the semiconductor Bloch equations.^{3,4} The semiconductor Bloch equations have been developed on different levels of complexity for the interaction of optically excited electron-hole pairs. They contain mean-field effects and correlations in the second-order Born approximation (SOBA) (Refs. 19–27) or in the coherent dynamics-controlled truncation scheme (DCTS).^{28–30} A description of the related quantum kinetic phenomena can be found in Ref. 4.

The DCTS is typically used in the weakly nonlinear intensity range to describe coherent phenomena, especially bound states, whereas the SOBA can be applied to a broad intensity range including the description of optical gain and Rabi flopping, at the expense of higher-order correlations such as biexcitons. Here, we use both techniques where they are appropriate in the description of pulse propagation phenomena. One should note that the overlap between both sets of equations occurs in the low-density regime, if higher-order correlation functions are neglected in the DCTS and the low-density limit is applied to the SOBA.

In the following we discuss the similarities and the differences of two-level systems and semiconductors more formally in terms of the corresponding equations of motion (compare Refs. 1–3). The reduced wave equation⁹ $(\partial/\partial z)\Omega(t, z) = -i\beta P(t, z)$ is used for the description of the field envelope E in form of the Rabi frequency $\Omega(t, z) = (d/\hbar)E(t, z)$ (d is the dipole moment). The source of the field is the polarization envelope P and β is a constant determined by material properties such as dipole moments and the refractive index. P is given by the off-diagonal density matrix element σ_{21} in the case of a two-level system $P = n_0 d \sigma_{21}$, where n_0 is the number density, and by all wave number transitions P_k in the case of a semiconductor $P = (d/V)\sum_k P_k$, where V is the sample volume. In the case of linear optics, σ_{21} is determined by a simple oscillator equation: $\dot{\sigma}_{21} = i\Delta\sigma_{21} + \frac{1}{2}i\Omega$ (Δ is the detuning). For semiconductors in the same limit, the equations for P_k can be diagonalized within the exciton basis to a similar form, where all exciton states λ contribute: $\dot{P}_\lambda = i\Delta_\lambda(z)P_\lambda + i\Omega_\lambda$. Restricting to the basic excitonic state $\lambda = 1s$, the material equations are formally identical, despite the fact that the dispersion $\Delta_{1s}(z)$ of the $1s$ exciton has to be taken into account. Thus,

in the case of linear optics, the material equations for two-level systems and excitons are formally similar and their coupling to the wave equation yields the discussed dispersion crossing of two oscillators. Despite modifications due to spatial dispersion in a semiconductor, both the two-level and semiconductor dynamics contain the temporal beating in the pulse tail described above.³¹

In the case of nonlinear optics of two-level systems, the only relevant nonlinearity is the Pauli-blocking nonlinearity $\dot{\sigma}_{21}|_{nl} = -i\Omega\sigma_{22}$, where σ_{22} is the transient occupation of the upper level. Without additional dephasing terms, the wave equation and the density matrix σ describe the vanishing polariton beating and the formation of pulse breakup due to Rabi flopping in two-level systems. Here, Rabi flopping is the transient oscillation of σ_{22} between occupation zero and one: $\sigma_{22}(t) = \sin^2[\Theta(t)/2]$. The pulse area $\Theta(t, z)$ is defined by the temporal integral over the Rabi frequency $\Omega(t, z)$: $\Theta(t, z) = \int_{-\infty}^t \Omega(t', z) dt' = (d/\hbar) \int_{-\infty}^t E(t', z) dt'$. The process of Rabi oscillation of the density leads to a temporal interplay of absorption and amplification for pulses having an area larger than or equal to 2π (high-intensity regime). In view of this, the coherent propagation of a resonant light pulse in a noninteracting two-level system is determined by the area theorem of McCall and Hahn.^{32,33} According to the area theorem, a light pulse with area $\Theta = 2\pi$ and hyperbolic secant envelope exhibits lossless soliton propagation on the resonance (SIT) due to an exact cancellation of the absorption and amplification process (one complete Rabi flop). For input areas larger than 3π , repeated Rabi oscillations cause pulse breakup into separate pulses with area of 2π . SIT and multiple pulse breakup were pioneered in atomic vapor about 30 years ago and have been thoroughly investigated in the 1970's.^{34–36}

Concerning the nonlinear optics of free excitons in a semiconductor, many-body effects have to be taken into account, which can be divided into mean-field and correlation effects. Mean-field effects consist not only of the Pauli-blocking contributions, but yield for the semiconductor coherent Coulomb renormalizations of the field as well as of the single-particle energies. For instance, the field renormalization is given by the Coulomb-mediated emission of all wave number transitions $\hbar\Omega_k = \frac{1}{2}dE + \sum_q V_{|k-q|} P_q$, where Ω_k is the generalized Rabi frequency and V_k is the Coulomb interaction. For subpicosecond to picosecond pulses in semiconductors such as CdSe or GaAs, this field correction almost doubles the Rabi frequency compared to two-level systems.^{11,12} As opposed to a noninteracting two-level system, one would therefore expect almost twice as many Rabi oscillations of the carrier density for a given pulse area. However, it must be noted that the number of Rabi flops for a 2π pulse in a semiconductor (yielding always one complete Rabi flop in a two-level system) varies as a function of the ratio of exciton binding energy and peak Rabi frequency³⁷ and care has to be taken in the interpretation of experiments. Numerical investigations of the corresponding semiconductor Bloch equations in mean-field approximation for the polarization coupled to Maxwell's wave equation for the propagating light field demonstrated Rabi flopping, co-

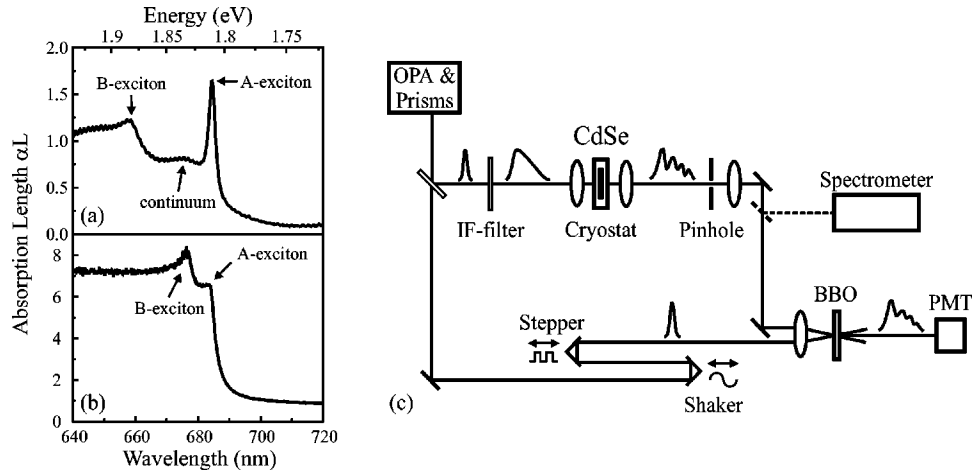


FIG. 1. (a),(b) Linear absorption spectra of the two CdSe samples at $T=8$ K. (a) Thin sample: $\alpha L=1.7$ at $\lambda_A=684.6$ nm. (b) Thick sample: $\alpha L=6.5$ at $\lambda_A=683.8$ nm. (c) Experimental setup using 60–70 fs pulses tunable around 684 nm from an optical parametric amplifier (OPA). The propagated pulses are time-resolved by cross correlation in a 2 mm thick β -barium-borate (BBO) crystal and detected with a photomultiplier tube (PMT).

herent long-distance propagation, and a high degree of transmission already for pulse areas larger than π .^{9,11,12} Lossless propagation—as in the case of SIT in two-level systems—was, however, excluded, even under idealized conditions where only mean-field effects are taken into account.

The next step of sophistication in treating the semiconductor material equations arises at the level where correlation effects are included. In principle, these effects cannot be neglected in nonlinear optics because they compensate some of the mean-field effects,^{19–27,38} especially energy shifts in stationary spectra. Using the SOBA, it can be recognized that within the course of time the correlations drive the system into a quasiequilibrium by carrier-carrier scattering and excitation-induced dephasing of the macroscopic polarization. For instance, in the weakly nonlinear regime and for a single circularly polarized pulse, the coupling of the one-exciton states to the free two-exciton continuum yields optical dephasing. At high densities, correlation effects reduce the coherent interaction effects such as exciton-polariton formation and Rabi oscillations. However, several experiments and theories have shown that coherent mean-field effects dominate the incoherent effects due to carrier-carrier scattering on sufficiently short time scales (compare the recent Ref. 39). As complete Rabi oscillations and SIT seem not to be possible in semiconductors, the associated pulse propagation phenomena are referred to as self-induced transmission.¹³

III. SAMPLES AND EXPERIMENTAL TECHNIQUES

The experiments were performed on two CdSe bulk crystals grown by hot-wall epitaxy on transparent BaF₂ substrates.⁴⁰ We used an optically thin sample with Beer absorption length $\alpha L=1.7$ to study propagation effects in the linear and the weakly nonlinear regime and an optically thick sample with $\alpha L=6.5$ to investigate the characteristics of high-intensity coherent nonlinear transmission. The c axis of CdSe was oriented perpendicularly to the substrate. Thus, both the intrinsic A - and B -exciton resonances could be ex-

cited with linearly polarized light normally incident to the samples ($\mathbf{E} \perp \mathbf{c}$). Figures 1(a) and 1(b) show the corresponding linear absorption spectra at $T=8$ K. The thin CdSe sample exhibits a well-defined A -exciton resonance at $\lambda_A=684.6$ nm with a full width at half maximum of approximately 3 nm. The large A -exciton binding energy $E_x=22.5$ meV (offset between A exciton and continuum) implies a large transition dipole moment and only weak interaction with the continuum states. The pronounced splitting of 72 meV between the A and B excitons can be attributed to strain in the CdSe layer due to lattice mismatch with the BaF₂ substrate and thermal expansion during the growth process.⁴¹ In the thick sample, however, strain relaxation prevented the occurrence of increased A - B exciton splitting. Additionally, the A -exciton resonance, situated at $\lambda_A=683.8$ nm, shows substantial inhomogeneous broadening.

Figure 1(c) illustrates the experimental setup. We used 60–70 fs pulses tunable around 684 nm with pulse energies of about 90 nJ from an optical parametric amplifier (OPA) (Ref. 42) pumped by a regenerative Ti:sapphire amplifier (COHERENT REGA) at a repetition rate of 200 kHz. Careful alignment of a prism compressor⁴³ made sure that the pulses were almost chirp-free, which was essential for the subsequent propagation experiment. The experimental configuration involves splitting of the linearly polarized OPA output into two portions: One part (67%) was additionally attenuated and focused with a $f=25$ mm microscope objective (Ealing, $NA=0.15$) onto the CdSe samples in a cold finger cryostat ($T=8$ K), while the second part (33%) passed through a variable delay line. We determined the spot size on the sample via knife-edge test and assumed an uncertainty of 20%. A first part of the transmitted pulses was spectrally recorded and a second part time-resolved by cross correlation with output pulses from the OPA in a 2 mm thick β -barium-borate (BBO) crystal cut for type I phase matching. The intensity cross-correlation signal may be written as

$$I_{\text{sig}}(\tau) \propto \int_{-\infty}^{\infty} I_{\text{trans}}(t) I_{\text{del}}(t-\tau) dt, \quad (3.1)$$

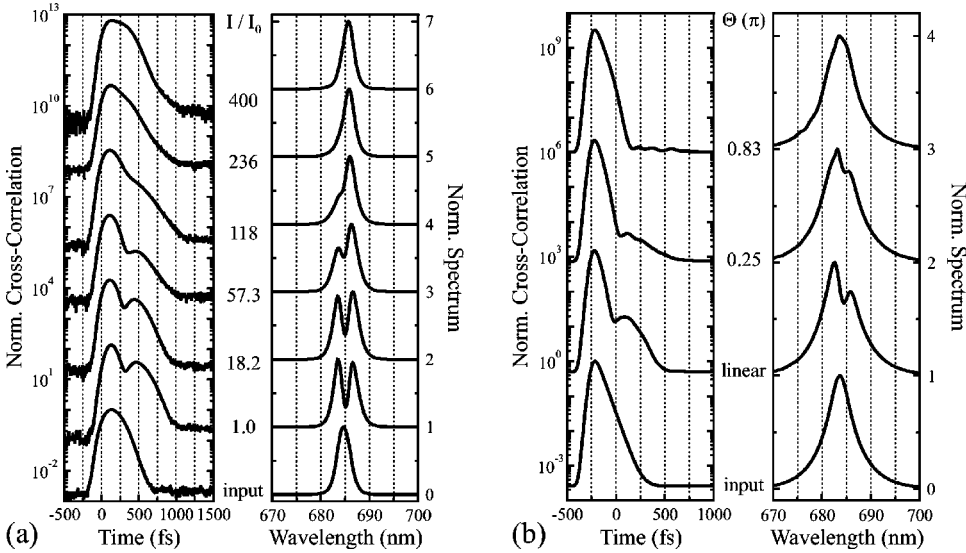


FIG. 2. (a) Propagation of 220 fs pulses through the thin CdSe sample with $\alpha L = 1.7$ for increasing intensities I . $\lambda = 684.6$ nm, $I_0 = 0.06$ MW/cm², and $T = 8$ K. The normalized cross-correlation traces are shown on a logarithmic scale at the left and the normalized transmitted spectra are plotted on a linear scale at the right. (b) Numerical simulation using the semiconductor Maxwell-Bloch equations in the dynamics-controlled truncation scheme.

where $I_{\text{trans}}(t)$ and $I_{\text{del}}(t)$ are the temporal profiles of the transmitted and the delayed pulses, and τ is the pulse delay. A fast-scan sampling technique was adopted to measure the cross-correlation signals: By means of the discrete translation of a stepper, we could calibrate the oscillation of a shaker, which in turn periodically modulated the pulse delay at a frequency of 70 Hz.⁴⁴ Thus, we achieved a high signal-to-noise ratio due to short measurement cycles and averaging over many (up to 4000) scans. Careful spectral and spatial filtering of the signal was found to be indispensable for the propagation experiment. Insertion of narrow bandpass filters (IF filters) before the cryostat adjusted the broad spectrum of the ultrashort OPA pulses to the A -exciton resonance of the CdSe samples. Thereby, the incident pulses were stretched up to 220 fs for 3 nm bandwidth and 800 fs for 1 nm bandwidth with roughly Lorentzian spectral shape. The theoretical assumption of spatially homogeneous wave fronts was approximated by imaging the transmitted beam onto a pin-hole, cutting out a region of constant intensity.

IV. RESULTS AND DISCUSSION

In this section, the transition from linear to nonlinear pulse propagation on the free-exciton resonance is discussed. Within this transition, two basic nonlinear effects are observed: The exciton-exciton interaction induced damping of the temporal polariton beating and the Rabi flopping related occurrence of temporal pulse breakup.

A. Excitation-induced suppression of temporal polariton beating

Figure 2(a) shows the experimental results of the propagation of 220 fs pulses resonantly tuned to the A -exciton resonance of the thin CdSe sample with $\alpha L = 1.7$ at $T = 8$ K. The left column illustrates the temporal cross-correlation traces of the transmitted pulses, whereas the right column shows the corresponding transmitted spectra behind the sample. The lowest traces characterize the input pulse as measured after propagation through the substrate alone. For

producing the input pulse, we made use of a spectral filter with 3 nm bandwidth to ensure that both branches of the polariton dispersion were coherently excited. In this manner, we obtained the above mentioned 220 fs pulses with roughly single-sided exponential envelope. Going from bottom to top in the figure, the pulse intensity is increasing from $I_0 = 0.06$ MW/cm² to $400 \times I_0 = 24$ MW/cm². The transmitted pulses indicate the expected temporal polariton beating in the linear propagation regime: Two distinct pulses, i.e., one full beat period, can be observed which are separated by approximately 340 fs. Further polariton beats are suppressed because of inhomogeneous broadening of the resonance and the short sample length.¹⁷ With increasing input intensity, the temporal beating decreases and almost vanishes at $118 \times I_0 = 7$ MW/cm². Simultaneously, the spectral dip (right column), which originates from the excitonic absorption, fades away. At an intensity of $236 \times I_0 = 14$ MW/cm², a shoulder with a delay of 270 fs with respect to the pulse maximum develops on the trailing edge of the transmitted pulse. Upon further increase of the intensity to $400 \times I_0 = 24$ MW/cm², the delay of the shoulder shortens to approximately 180 fs. At the same time, the transmitted spectra resemble the input spectrum and do not broaden, ruling out any perturbing influence of self-phase modulation (SPM) (Ref. 45) from off-resonant states or the substrate.

A theoretical model capable of explaining our experimental observations, especially the suppression of the polariton beating, was developed recently¹⁷ on the basis of the semiconductor Maxwell-Bloch equations in the DCTS (see Sec. II). This model can only be applied for the weakly nonlinear regime discussed here. The material equations were evaluated for plane-wave propagation using a tight-binding approximation for the band structure and one-dimensional Coulomb interaction.³⁸ Inhomogeneous broadening of the resonance due to sample strain was additionally included in the model by averaging the polarization calculated for Gaussian-distributed band gap energies. Parameters for the CdSe material are given in Ref. 46. For comparison with the experiment, the computed time-resolved signals were con-

volved with a 50 fs Gaussian pulse according to Eq. (3.1). The initial pulse had a duration of 180 fs with a single-sided exponential envelope. Results of the numerical simulation are depicted in Fig. 2(b). For linear excitation, a single polariton beat can be observed about 310 fs after the pulse maximum. At higher excitation densities, the theoretical cross-correlation traces exhibit the anticipated suppression of the polariton beating both temporally and spectrally in full agreement with our experiment.

The theoretical analysis shows that only one polariton beat period is found at low intensities because beating at longer times is suppressed due to the inhomogeneous broadening of the resonance. At increasing intensities, the excitonic polarization is dephased caused by the coupling of excitons to unbound two-exciton states, i.e., to an interaction-generated continuum. The observed shoulder at highest intensities [Fig. 2(a)] indicates a regime with higher-order nonlinearities. The forming of the shoulder is a manifestation of the beginning of a first carrier density Rabi flop, with the latter occurring at a higher frequency when the light field is intensified. Indeed, we find a shorter delay of the shoulder with respect to the pulse maximum for the higher pulse intensity. However, for increasing intensities, coherent pulse breakup cannot reveal itself clearly in such a thin sample^{1,47} and the low-intensity DCTS breaks down at sufficiently high carrier densities. The cross correlation of a 200 fs pulse with a 50 fs pulse is another limiting factor since it smears out the fine structure when Rabi flopping induced pulse breakup exhibits more than one minimum. Furthermore, the effects of Rabi flopping induced pulse breakup become much more pronounced for longer propagation distances.¹³ For these reasons, we choose a thicker sample as well as a longer pulse duration and higher pulse intensities to investigate pulse breakup due to Rabi flopping. Correspondingly, the theoretical description is carried out within the SOBA.

B. Self-induced transmission and multiple pulse breakup

Using the thick sample with $\alpha L = 6.5$ in the following studies, we turn our attention to the high-excitation regime exclusively. Low-intensity light will no longer propagate through the sample since the linear transmission is only 0.15%. We utilized a 1 nm bandwidth filter in order to excite a narrow distribution of transitions within the *A*-exciton resonance, thus reducing the influence of inhomogeneous broadening and of the cross-correlation measurement. Figure 3 demonstrates that coherent nonlinear propagation is indeed observable on the initial pulse shape at high pulse intensities. Again, the plot shows temporal cross-correlation traces for increasing intensities from bottom to top. The lowest trace illustrates the roughly single-sided exponential input pulse with 800 fs duration. At an intensity $I_0 = 105 \text{ MW/cm}^2$, the pulse transmitted through the sample is already steepened, shortened, and shows a higher symmetry compared with the original pulse shape. On closer inspection, the trace exhibits a slight shoulder structure about 550 fs after the maximum. In addition, a large delay of approximately 700 fs is measured with respect to the input pulse (evaluated at 50% of the normalized signal height between the rising pulse edges).

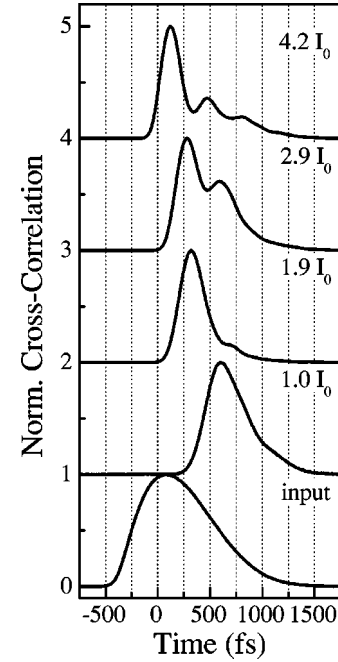


FIG. 3. Propagation of 800 fs pulses through the thick CdSe sample with $\alpha L = 6.5$ for increasing intensities I . $\lambda = 683 \text{ nm}$, $I_0 = 105 \text{ MW/cm}^2$, and $T = 8 \text{ K}$. The normalized cross-correlation traces are shown on a linear scale.

Increasing the intensity to $1.9 \times I_0 = 200 \text{ MW/cm}^2$, the pulse reshaping and the shoulder structure become even more pronounced. Both, the temporal distance between the two pulse components and the pulse delay reduce to approximately 400 and 470 fs, respectively. Upon further increase of the intensity to $2.9 \times I_0 = 305 \text{ MW/cm}^2$ and $4.2 \times I_0 = 440 \text{ MW/cm}^2$, distinct pulse breakups into several individual pulses are observed. At $2.9 \times I_0$, the intensified second pulse is emitted about 320 fs after the main pulse component, and approximately 1000 fs after the maximum, a small third shoulder develops. At $4.2 \times I_0$, three succeeding peaks are clearly visible, which appear about 350, 690, and 1040 fs after the first peak. As shown later, the pulse breakup is related to Rabi oscillations. In a simple model based on the two-level solution for σ_{22} and using $E \propto \sqrt{I}$, one expects the dynamics of the pulse breakup to be roughly twice as fast at four times the intensity. The number of peaks is correct, and the re-emission frequency grows by a factor of 1.6 within the covered intensity range. Moreover, the experimental results show that the delay between the transmitted and the original pulses further reduces with increasing intensity. This subject will be quantitatively discussed below. At the input intensity of $4.2 \times I_0$, we measured a total nonlinear transmission through the sample (corrected for surface reflectivity) greater than 25%. Behind the pinhole, which was inserted to restrict the signal detection to directly propagated and spatially homogeneous wave fronts, the transmission degree reached 6.25% compared to a linear transmission of merely 0.15% for $\alpha L = 6.5$. In combination with these nonlinear transmission values, the data of Fig. 3 prove the presence of self-induced transmission and multiple pulse breakup due to coherent carrier density Rabi flopping.

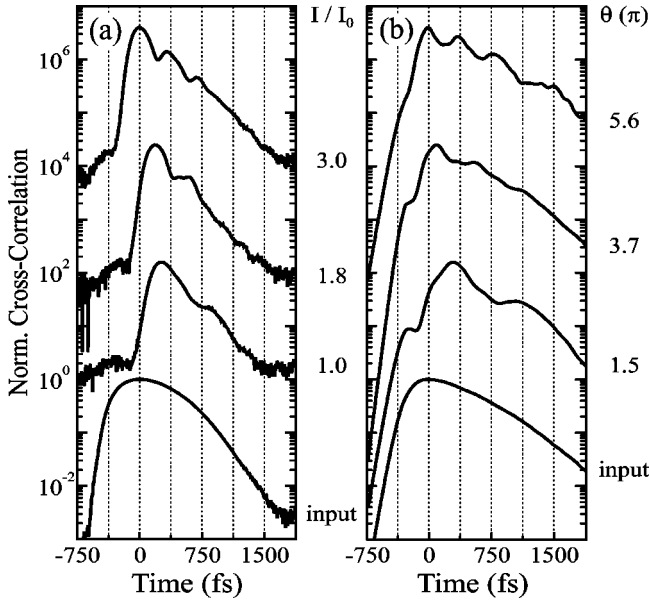


FIG. 4. (a) Propagation of 800 fs pulses through the thick CdSe sample with $\alpha L = 6.5$ for increasing intensities I . $\lambda = 683$ nm, $I_0 = 150$ MW/cm², and $T = 8$ K. The normalized cross-correlation traces are shown on a logarithmic scale. (b) Numerical simulation using the semiconductor Maxwell-Bloch equations in the second-order Born approximation.

In order to analyze the high-intensity dynamics in more detail, we plotted traces transmitted through the thick sample on a logarithmic scale [Fig. 4(a)]. Note that this set of traces differs from that in Fig. 3, but demonstrates the excellent reproducibility of our experimental data. Figure 4(b) shows the results of numerical calculations based on the semiconductor Maxwell-Bloch equations. Here, we applied the slowly varying envelope approximation (SVEA) of the field equation for numerical simplicity,⁹ whereas the material equations include mean-field and correlation effects (diagonal and nondiagonal dephasing as well as nonlinear polarization scattering) in the SOBA for polarization and carrier distribution.^{19–27} The resulting material equations are a standard tool in semiconductor optics. For the CdSe material, we used parameters given in Ref. 46, except for the inhomogeneous broadening which is numerically not tractable because of the long propagation distance and the more involved material equations. However, we believe that due to the longer pulse width, inhomogeneous broadening is of minor importance. The theoretical analysis shows that the pulse breakup can be traced back to Rabi flopping of the carrier density in a highly excited semiconductor. Increasing the intensity corresponds to a higher Rabi oscillation frequency and therefore to a faster interplay of absorption and emission in the course of time, which modulates the pulse shape. Our theoretical investigations yield that carrier-carrier scattering on the time scale of the pulse duration is of minor importance in comparison to mean-field effects which cover the main physics, similar to the recent results presented in Ref. 39.

In Fig. 4(a), we observe intensity-dependent multiple pulse breakup comparable to the behavior in Fig. 3. The lowest input intensity is $I_0 = 150$ MW/cm². Interestingly, the

second Rabi flop for $1.8 \times I_0 = 270$ MW/cm² shows a double substructure which is reproduced by the numerical simulation involving many-body interactions for a pulse area $\Theta = 3.7\pi$. Note that only the curves for $1.8 \times I_0 = 270$ MW/cm² and $\Theta = 3.7\pi$ are directly comparable in this figure. According to $\Theta \propto E \propto \sqrt{I}$, $\Theta = 1.5\pi$ corresponds to $0.3 \times I_0$ and 5.6π corresponds to $4.1 \times I_0$. Thus, the calculated traces represent the limits wherein the experimental curves are set. The breakup into two pulses is reproduced for the lowest input intensity $I_0 = 150$ MW/cm² and an area of 1.5π , respectively. Owing to the fact that the input pulse shape of the numerical model differs slightly from the experimental input pulse, the second peak is more pronounced in the theory. Also, the temporal distance with respect to the maximum is smaller in the experiment because of the higher excitation density, which results in a larger Rabi frequency and therefore faster reemission from the sample. For a pulse area $\Theta = 5.6\pi$, the calculated transmitted pulse shows four separate peaks, whereas the experimental trace indicates breakup into only three individual pulses. Most likely, the fourth pulse is already eliminated due to increased incoherence in the sample, contrary to the measurement series depicted in Fig. 3. The temporal spacing between the maximum and the succeeding peaks is roughly the same as can be seen when comparing the upper curves in Figs. 4(a) and 4(b), showing that the many-body calculation is able to produce the correct pulse velocity over a long propagation distance in a broad range of intensities. Precursors, which are purely propagation induced, can be seen both experimentally and theoretically for each excitation density.

Clearly observable in experiment and theory is the reduced delay between transmitted and input pulses for increased light intensities, indicating that the dynamical response of the matter emerges earlier due to the larger pulse area and higher Rabi frequency. In turn, this implies the definition of a higher effective propagation velocity v_{eff} through the sample: $v_{\text{eff}} = L / (\tau_{1/2} + L/c_0)$. Here, $\tau_{1/2}$ is the pulse delay measured at 50% of the maximum signal height between the rising edges of the transmitted and the input pulses and L is the sample thickness derived from the absorption length αL . Assuming an absorption coefficient $\alpha \approx 1 \mu\text{m}^{-1}$,⁴⁸ L is approximately $6.5 \mu\text{m}$ for the thick sample ($\alpha L = 6.5$). The pulse delay and the effective velocity are plotted versus input intensity in Fig. 5. The delay decreases from 840 fs for $I = 78$ MW/cm² to below 400 fs for $I = 400$ MW/cm². The corresponding effective velocity v_{eff} is ranging from $0.025 c_0$ to $0.052 c_0$. In the literature for coherent nonlinear propagation in isolated two-level systems,^{1,33} we find an estimate for the propagation velocity of 2π solitons $v_{\text{eff}} = c_0 / (n + \frac{1}{2} \alpha \tau_p c_0)$. For a pulse duration $\tau_p = 800$ fs, the absorption coefficient from above, and the refractive index $n = \sqrt{\epsilon_b}$ with the background dielectric constant $\epsilon_b \approx 9$ for our material,⁴⁸ a velocity of $v_{\text{eff}} = 0.0081 c_0$ is calculated in this model. Considering the mean-field correction for the excitonic many-body system (see Sec. II), we expect a comparable velocity for a π pulse in our semiconductor system (one complete Rabi flop). Extrapolating the intensity-dependent velocity curve to around 25 MW/cm², corre-

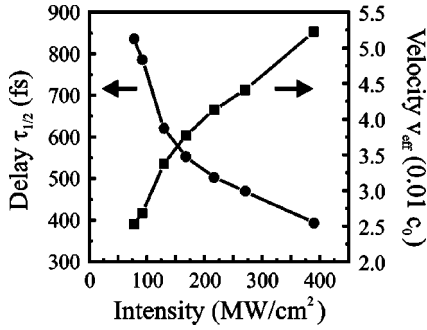


FIG. 5. Delay $\tau_{1/2}$ and effective propagation velocity v_{eff} for the propagation of 800 fs pulses through the thick CdSe sample with $\alpha L = 6.5$ at various input intensities I . $\lambda = 683$ nm and $T = 8$ K.

sponding to an area of about π (as shown below), one would obtain a velocity in the range of 0.015 to 0.02 c_0 . This velocity is quite low and means that the light is absorbed into the excited state and reemitted subsequently with an intensity dependent delay given by the Rabi frequency. More elaborate, but different experiments in atomic three-level systems have recently perfected the slowdown to a complete halt of the light.^{49,50}

The simplified model which describes the dynamics of the pulse breakup allows one to directly relate measured pulse intensities I to calculated pulse areas Θ . Due to the mean-field correction, breakup into two (four) individual pulse components is supposed to occur for incident 2π (4π) pulses. With respect to the measurement series depicted in Fig. 3, using $\Theta \propto \sqrt{I}$, we obtain an intensity of approximately 27 MW/cm² for an area of π . Comparing experimental and simulated pulse traces in Fig. 4, where the features of the $1.8 \times I_0 = 270$ MW/cm² curve are very well reproduced by the theoretical curve calculated for a pulse area of 3.7π , we deduce $I \approx 20$ MW/cm² for $\Theta = \pi$. Thus, an intensity of about 25 MW/cm² corresponds to an area of π for an 800 fs pulse in a CdSe sample with $\alpha L = 6.5$. Since the measured external intensity $I = \frac{1}{2} \sqrt{\epsilon_0 / \mu_0} (E_{\text{out}})^2$ and the internal pulse area $\Theta \approx (d/\hbar) E_{\text{in}} \tau_p$, where the relation between the electric field envelope inside and outside the sample is given by the Fresnel formula $E_{\text{in}}/E_{\text{out}} = 2/(n+1)$ with the refractive index $n \approx 3$, the dipole moment amounts to $d = 3.8$ eÅ. Taking the literature value for the longitudinal-transverse splitting energy of the A exciton in CdSe $\Delta_{\text{LT}} = 0.9$ meV (compare Ref. 48) and using the relation $\Delta_{\text{LT}} = (2d^2)/(\epsilon_b \epsilon_0 a_B^3)$ [derived from Eq. (11.10) in Ref. 3] with the exciton Bohr radius $a_B = 53$ Å for an A -exciton binding energy $E_x = 15$ meV and the background dielectric constant $\epsilon_b = 9$, the dipole moment is calculated to be $d = 1.8$ eÅ. Considering the uncertainty in quantifying the applied intensity and in relating this intensity to pulse area, the agreement is fairly good. It will be interesting to investigate the exact influence of the mean-field correction on the pulse area required for self-induced transmission.³⁷

Next, we discuss the influence of self-induced transmission on the spectral shape of the propagated pulses. Figures 6(a) and 6(b) depict the transmitted spectra for low and high input intensities (150 and 450 MW/cm² with $\Theta = 1.5\pi$ and 5.6π , respectively). At low intensities, the spectra represent

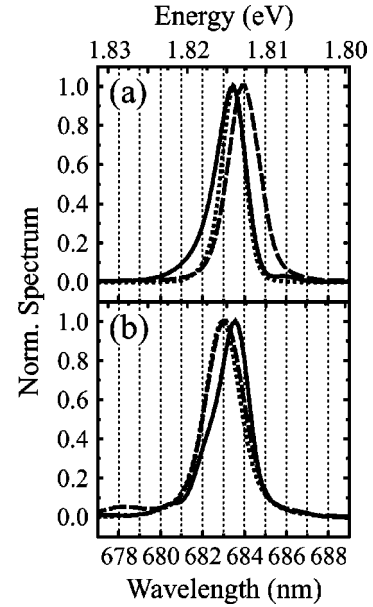


FIG. 6. Transmitted spectra corresponding to the resonant propagation of 800 fs pulses through CdSe at low and high intensities in the regime of self-induced transmission. The normalized spectra are plotted on a linear scale with respect to the input spectrum (dotted line). (a) Experiment: Thick sample with $\alpha L = 6.5$ at $T = 8$ K, $\lambda = 683.5$ nm, $I = 150$ MW/cm² (dashed line) and 450 MW/cm² (solid line). (b) Theory: Numerical calculations using the semiconductor Maxwell-Bloch equations in the second-order Born approximation, $\Theta = 1.5\pi$ (dashed line) and 5.6π (solid line).

symmetrical peaks in the experiment as well as in theory. While the transmitted spectrum roughly coincides with the input spectrum in theory, the experimental curve is slightly shifted and broadened towards the low-energy side. The shift is certainly due to detuning of the excitation against the resonance in the experiment as the maximum of the transmitted spectrum is found to be located exactly on the edge of the inhomogeneously broadened A -exciton resonance of the thick sample ($\lambda_A = 683.8$ nm). The spectral broadening emerges from spectral components at the low-energy side of the resonance that do not interact with the system. At high intensities, the transmitted spectra are asymmetrically broadened: The high- and low-energy sides show a slowly decaying tail and a steep edge, respectively. Modulations occur in the wings of the spectra, probably caused by the temporal modulation which leads to the pulse breakup. In contrast to the good agreement of the spectral shape between experiment and theory, the peak shifts of the spectra have opposite sign. We believe that this behavior originates from the detuning towards higher energies in the experiment. At low intensities, reemission of light following the temporal evolution of the excitonic polarization occurs on the edge of the A -exciton resonance, featuring the highest transition dipole moment. However, for increasing intensity, the exciting light field governs the spectral range within the inhomogeneously broadened exciton resonance where coherent Rabi flopping proceeds. Thus, the theoretically predicted redshift could not be observed in the experiment.

The fact that we do not observe spectral broadening at higher intensities and in the case of pulse breakup is a strong indication against SPM due to other transitions than the considered free excitons. This can be quantified by using the simplified formula⁴⁵ $\Delta\Phi = (2\pi/\lambda)n_2IL$ with the nonlinear refractive index $n_2 \approx 10^{-12} \text{ cm}^2/\text{W}$ for the CdSe bulk material,⁵¹ $I \approx 25 \text{ MW}/\text{cm}^2$ for a pulse area $\Theta = \pi$, $L \approx 6.5 \text{ }\mu\text{m}$ for the thick sample, and $\lambda = 683.8 \text{ nm}$. We obtain a nonlinear phase shift of $\Delta\Phi \approx 1.5 \text{ mrad}$, which is two orders of magnitude less than the phase shift of 0.2 rad required for SPM.⁵²

The data presented in this chapter provide clear evidence for long-distance coherent pulse propagation and high nonlinear transmission due to Rabi oscillations on the *A*-exciton resonance in CdSe for pulse areas up to a multiple of π . In agreement with theoretical predictions, this finding demonstrates that even for excitation intensities in the range of $100 \text{ MW}/\text{cm}^2$, substantial coherence between the exciting laser field and the excitonic polarization is maintained over several hundred femtoseconds despite many-body interaction effects. Consequently, excitation-induced dephasing is less important in progress of the applied pulses on the ultrashort time scale considered here.

C. Phonon-induced dephasing of the excitonic polarization

In order to investigate the influence of enhanced phase relaxation on the features of self-induced transmission, we have performed pulse propagation experiments at varying sample temperature. If the temperature is increased, phase-destroying electron/hole-phonon scattering occurs that, for our purposes, primarily reduces the amplitude of the excitonic polarization and the coherent interaction during the duration of the pulse. The contribution of phonon scattering to phase relaxation grows linearly with T in the range where acoustic phonon scattering dominates and even superlinearly for temperatures which permit optical phonon scattering.^{53,54}

Figure 7 presents cross-correlation traces for 800 fs pulses transmitted through the thick CdSe sample ($\alpha L = 6.5$) for varying intensities and temperatures. In the horizontal direction, the intensity is varied from $I_0 = 105 \text{ MW}/\text{cm}^2$ to $4.2 \times I_0 = 440 \text{ MW}/\text{cm}^2$, corresponding to a doubling of the external electric field and the Rabi frequency, respectively. In the vertical direction, the temperature is raised from bottom to top from 10 to 70 K. The set of data in the bottom line depicts the development of coherent multiple pulse breakup as already discussed above. The right column (highest intensity) shows a remarkable reduction of the modulation depth with rising temperature. Notice that the decay of the modulation depth with time caused by dephasing processes is strongly enhanced for higher temperatures because of the additional contribution of exciton-phonon scattering. For the highest intensity trace at $T = 70 \text{ K}$ (upper right), the pulse is still transmitted, but the pulse breakup has almost completely vanished. Only a weak second peak is barely visible. The coherently propagated amount of light evidently has dropped compared to the value at $T = 10 \text{ K}$ owing to the interaction with phonons which dephases the coherent polarization and supports the buildup of an incoherent exciton population.⁵⁵

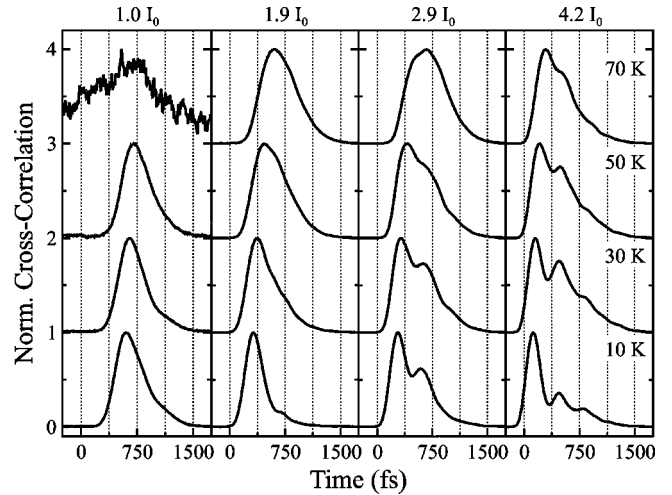


FIG. 7. Propagation of 800 fs pulses through the thick CdSe sample with $\alpha L = 6.5$ for increasing intensities I (horizontal direction) and increasing temperature T (vertical direction). $\lambda = 683 \text{ nm}$ and $I_0 = 105 \text{ MW}/\text{cm}^2$. The normalized cross-correlation traces are shown on a linear scale.

Thus, the dominant part of the transmission originates from incoherent bleaching of the exciton transition, which explains the increased unmodulated background level. Similarly, the dominance of the exciton-phonon coupling over the exciton-light coupling arises from the growing delay between the input and the transmitted pulses for elevated temperatures. The effect is reproduced in every single column, however, phase relaxation due to phonon scattering manifests itself more strongly at lower input intensities where the importance of the exciton-phonon interaction is enhanced in comparison with the exciton-light coupling.

The observations discussed in this section are certainly not caused by the redshift of the *A*-exciton resonance of approximately 9 meV within the viewed temperature range. Due to the inhomogeneously broadened resonance of the thick sample, detuning experiments at $T = 10 \text{ K}$ with the excitation shifted towards higher energies by more than 7 meV showed only little influence on the features of coherent multiple pulse breakup.

V. CONCLUSIONS

We have presented a comprehensive study of subpicosecond pulse propagation on the *A*-exciton resonance in bulk CdSe. At low pulse intensities, polariton formation and the corresponding interference effects result in temporal polariton beating. The linear polariton concept begins to fail at higher excitation densities where the polariton beating is suppressed in consequence of incoherent exciton-exciton interaction which causes dephasing of the excitonic polarization. Self-induced transmission and coherent multiple pulse breakup due to Rabi flopping of the carrier density are prominent at pulse areas beyond π . At intensities on the order of $100 \text{ MW}/\text{cm}^2$, tight coherent control of the temporal evolution of the excitonic polarization by the applied ultrashort pulse results in a large amount of coherent nonlinear

transmission and a high contrast ratio of the pulse breakup. The experiments can be described theoretically using the semiconductor Maxwell-Bloch equations, which accomplish the transition from linear to nonlinear optics by taking into account many-body interactions consisting of mean-field and correlation effects. Further findings such as the intensity to pulse area relation as well as pulse delays and effective propagation velocities in dependence on the pulse intensity yield quantitative agreement between the experiment and the semiconductor Maxwell-Bloch theory. Increasing the phase relaxation rate by introducing exciton-phonon scattering at elevated sample temperatures greatly diminishes the amplitude of the coherent excitonic polarization, thus gradually

destroying the contrast ratio of the Rabi flopping induced pulse breakup.

ACKNOWLEDGMENTS

We would like to thank W. W. Rühle and B. Hillebrands for continuous support. We are grateful to F. Widulle for a critical reading of the manuscript. The high-quality samples were grown by M. Grün and M. Hetterich in the group of C. Klingshirn. Financial support came from the Deutsche Forschungsgemeinschaft through the Graduiertenkolleg "Optoelektronik mesoskopischer Halbleiter" and through the Quantenkohärenzschwerpunkt.

- *Present address: Institute of Applied Physics, University of Bonn, D-53115 Bonn, Germany.
- ¹L. Allen and J. H. Eberly, *Optical Resonance and Two-Level Atoms* (Dover Publications, New York, 1987).
 - ²M. O. Scully and M. S. Zubairy, *Quantum Optics* (Cambridge University Press, New York, 1997).
 - ³H. Haug and S. W. Koch, *Quantum Theory of the Optical and Electronic Properties of Semiconductors* (World Scientific Publishing, Singapore, 1993).
 - ⁴H. Haug and A. P. Jauho, *Quantum Kinetics in Transport and Optics of Semiconductors* (Springer-Verlag, Berlin, 1996).
 - ⁵C. F. Klingshirn, *Semiconductor Optics* (Springer-Verlag, Berlin, 1997).
 - ⁶Phys. Status Solidi B **159**, (1990); **173**, (1992); **188**, (1995); **206**, (1998); **221**, (2000).
 - ⁷M. Jütte, H. Stolz, and W. von der Osten, J. Opt. Soc. Am. B **13**, 1205 (1996).
 - ⁸V. M. Agranovich and V. L. Ginzburg, *Crystal Optics with Spatial Dispersion and Excitons*, Vol. 42 of Springer Series in Solid-State Sciences (Springer-Verlag, Berlin, 1984).
 - ⁹A. Knorr, R. Binder, M. Lindberg, and S.W. Koch, Phys. Rev. A **46**, 7179 (1992).
 - ¹⁰I. Talanina, D. Burak, R. Binder, H. Giessen, and N. Peyghambarian, Phys. Rev. E **58**, 1074 (1998).
 - ¹¹R. Binder, S.W. Koch, M. Lindberg, N. Peyghambarian, and W. Schäfer, Phys. Rev. Lett. **65**, 899 (1990).
 - ¹²S.W. Koch, A. Knorr, R. Binder, and M. Lindberg, Phys. Status Solidi B **173**, 177 (1992).
 - ¹³H. Giessen, A. Knorr, S. Haas, S.W. Koch, S. Linden, J. Kuhl, M. Hetterich, M. Grün, and C. Klingshirn, Phys. Rev. Lett. **81**, 4260 (1998).
 - ¹⁴J.J. Hopfield, Phys. Rev. **112**, 1555 (1958).
 - ¹⁵D. Fröhlich, A. Kulik, B. Uebbing, A. Mysyrowicz, V. Langer, H. Stolz, and W. von der Osten, Phys. Rev. Lett. **67**, 2343 (1991).
 - ¹⁶D. Fröhlich, A. Kulik, B. Uebbing, V. Langer, H. Stolz, and W. von der Osten, Phys. Status Solidi B **173**, 31 (1992).
 - ¹⁷J. Förstner, A. Knorr, S. Kuckenburger, T. Meier, S.W. Koch, H. Giessen, S. Linden, and J. Kuhl, Phys. Status Solidi B **221**, 453 (2000).
 - ¹⁸D.S. Kim, J. Shah, D.A.B. Miller, T.C. Damen, W. Schäfer, and L. Pfeiffer, Phys. Rev. B **48**, 17 902 (1993).
 - ¹⁹M. Lindberg and S.W. Koch, Phys. Rev. B **38**, 3342 (1988).
 - ²⁰T. Rappen, U.G. Peter, M. Wegener, and W. Schäfer, Phys. Rev. B **49**, 10 774 (1994).
 - ²¹W. Schäfer, I. Brener, and W. Knox, in *Coherent Optical Interactions in Semiconductors*, edited by R. T. Philipps (Plenum Press, New York, 1994), p. 343.
 - ²²F. Rossi, S. Haas, and T. Kuhn, Phys. Rev. Lett. **72**, 152 (1994).
 - ²³E. Heiner, Phys. Status Solidi B **153**, 295 (1989).
 - ²⁴W. Pötz, Phys. Rev. B **54**, 5647 (1996).
 - ²⁵F. Jahnke, M. Kira, S.W. Koch, G. Khitrova, E.K. Lindmark, T.R. Nelson, Jr., D.V. Wick, J.D. Berger, O. Lyngnes, H.M. Gibbs, and K. Tai, Phys. Rev. Lett. **77**, 5257 (1996).
 - ²⁶A. Knorr, S. Hughes, T. Stroucken, and S.W. Koch, Chem. Phys. **210**, 27 (1996).
 - ²⁷F. Jahnke, M. Kira, and S.W. Koch, Z. Phys. B **104**, 559 (1997).
 - ²⁸V.M. Axt and A. Stahl, Z. Phys. B **93**, 195 (1994).
 - ²⁹M. Lindberg, Y.Z. Hu, R. Binder, and S.W. Koch, Phys. Rev. B **50**, 18 060 (1994).
 - ³⁰W. Schäfer, D.S. Kim, J. Shah, T.C. Damen, J.E. Cunningham, K.W. Goossen, L.N. Pfeiffer, and K. Köhler, Phys. Rev. B **53**, 16 429 (1996).
 - ³¹D.C. Burnham and R.Y. Chiao, Phys. Rev. **188**, 667 (1969).
 - ³²S.L. McCall and E.L. Hahn, Phys. Rev. Lett. **18**, 908 (1967).
 - ³³S.L. McCall and E.L. Hahn, Phys. Rev. **183**, 457 (1969).
 - ³⁴H.M. Gibbs and R.E. Slusher, Phys. Rev. Lett. **24**, 638 (1970).
 - ³⁵R.E. Slusher and H.M. Gibbs, Phys. Rev. A **5**, 1634 (1972).
 - ³⁶R.E. Slusher and H.M. Gibbs, Phys. Rev. A **6**, 1255(E) (1972).
 - ³⁷Th. Östreich and A. Knorr, Phys. Rev. B **48**, 17 811 (1993).
 - ³⁸C. Sieh, T. Meier, A. Knorr, F. Jahnke, P. Thomas, and S.W. Koch, Eur. Phys. J. B **11**, 407 (1999).
 - ³⁹M. Saba, F. Quochi, C. Ciuti, D. Martin, J.L. Staehli, B. Deveaud, A. Mura, and G. Bongiovanni, Phys. Rev. B **62**, R16322 (2000).
 - ⁴⁰M. Grün, M. Hetterich, U. Becker, H. Giessen, and C. Klingshirn, J. Cryst. Growth **141**, 68 (1994).
 - ⁴¹U. Becker, H. Giessen, F. Zhou, Th. Gilsdorf, J. Loidolt, M. Müller, M. Grün, and C. Klingshirn, J. Cryst. Growth **125**, 384 (1992).
 - ⁴²M.K. Reed, M.K. Steiner-Shepard, M.S. Armas, and D.K. Negus, J. Opt. Soc. Am. B **12**, 2229 (1995).
 - ⁴³R.L. Fork, O.E. Martinez, and J.P. Gordon, Opt. Lett. **9**, 150 (1984).
 - ⁴⁴D.C. Edelstein, R.B. Romney, and M. Scheuermann, Rev. Sci. Instrum. **62**, 579 (1991).
 - ⁴⁵J. C. Diels and W. Rudolph, *Ultrashort Laser Pulse Phenomena* (Academic Press, San Diego, 1996), p. 140.
 - ⁴⁶The CdSe material was modelled with a gap energy $E_g = 1.85$ eV, a tight binding band width energy $\Delta_p = 35.2$ meV, an

- exciton binding energy $E_x=15$ meV, a longitudinal-transverse splitting energy $\Delta_{\text{LT}}=1$ meV, an effective electron and hole mass $m_e=0.125 m_0$ and $m_h=0.431 m_0$, a background dielectric constant $\epsilon_b=9$, and an absorption coefficient $\alpha=1 \mu\text{m}^{-1}$. A value of 6 meV was assumed for the inhomogeneous broadening of the resonance.
- ⁴⁷G.L. Lamb, Jr., *Rev. Mod. Phys.* **43**, 99 (1971).
- ⁴⁸Landolt-Börnstein, *Numerical Data and Functional Relationships in Science and Technology*, New Series, Group III, Vol. 17b, edited by I. Broser, R. Broser, and A. Hoffmann (Springer-Verlag, Berlin, 1982), pp. 202, 442.
- ⁴⁹D.F. Phillips, A. Fleischhauer, A. Mair, R.L. Walsworth, and M.D. Lukin, *Phys. Rev. Lett.* **86**, 783 (2001).
- ⁵⁰C. Liu, Z. Dutton, C.H. Behroozi, and L.V. Hau, *Nature (London)* **409**, 490 (2001).
- ⁵¹B.S. Wherrett, A.C. Walker, and F.A.P. Tooley, *Nonlinear Refraction for CW Optical Bistability*, in *Optical Nonlinearities and Instabilities in Semiconductors*, edited by H. Haug (Academic Press, New York, 1988), p. 244.
- ⁵²B.J. Eggleton, G. Lenz, R.E. Slusher, and N.M. Litchinitser, *Appl. Opt.* **37**, 7055 (1998).
- ⁵³L. Schultheis, A. Honold, J. Kuhl, K. Köhler, and C.W. Tu, *Phys. Rev. B* **34**, 9027 (1986).
- ⁵⁴J. Lee, E.S. Koteles, and M.O. Vassell, *Phys. Rev. B* **33**, 5512 (1986).
- ⁵⁵A. Thranhardt, S. Kuckenburger, A. Knorr, T. Meier, and S.W. Koch, *Phys. Rev. B* **62**, 2706 (2000).